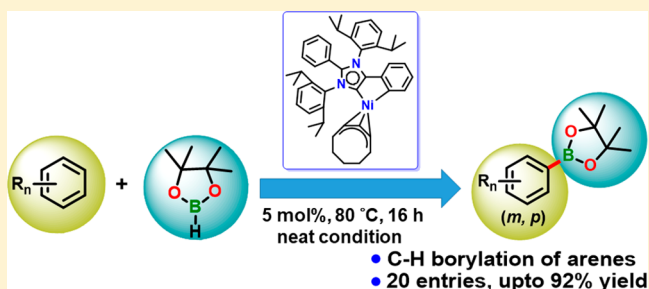


Nickel-Catalyzed C(sp²)–H Borylation of ArenesArpan Das, Pradip Kumar Hota, and Swadhin K. Mandal*^{id}

Department of Chemical Sciences, Indian Institute of Science Education and Research Kolkata, Mohanpur 741246, India

Supporting Information

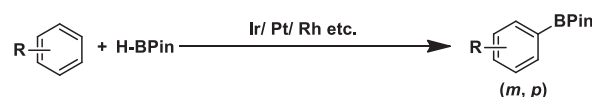
ABSTRACT: In this study, C(sp²)–H borylation of arenes was accomplished by a nickel catalyst, resulting in good yield. Alkyl and alkoxy arenes were successfully functionalized, affording C(sp²)–H borylated compounds. It was unraveled that the well-defined abnormal N-heterocyclic carbene based Ni(II) complex breaks into Ni nanoparticles (Ni-NPs), which act as catalytically active species. A series of controlled reactions under stoichiometric conditions along with spectroscopic studies and single-crystal X-ray crystallographic study helped us to understand the formation of Ni-NPs along with formation of a boron(III) compound during this reaction.



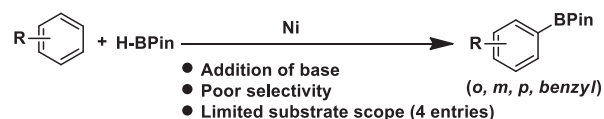
Organoboron compounds are considered as extremely useful reagents in organic synthesis, since they are important synthons to prepare various core moieties of pharmaceutically important molecules,¹ natural products,² and organic materials.³ Apart from the transition-metal-catalyzed coupling of aryl halides or pseudohalides with boronyl esters, the direct functionalization of C–H bonds using a borane source is one of the most effective methods to synthesize such compounds.^{4,5} The direct C–H bond functionalization has several benefits in comparison to conventional synthetic routes for the preparation of aryl boronates. In this method, prefunctionalized arenes are not needed, making this process more atom economical and cheaper. In this context, transition-metal-catalyzed C(sp²)–H borylation of arenes has come to the limelight in modern catalysis, as it helps to introduce a synthetically important boron moiety directly into an aromatic ring in absence of any directing group. Earlier, [Ir(COD)(OMe)]₂ (COD = 1,5-cyclooctadiene) and [Ir(COE)(OMe)]₂ (COE = cyclooctene) in association with an organic ligand such as bipyridine or phenanthroline have been extensively used for such transformations due to their high activity and good functional group tolerance.⁶ Later on, the versatility of the iridium catalysts encouraged many others to explore the activity of iridium-, rhodium-, and platinum-based catalysts under homogeneous conditions as well as heterogeneous conditions toward the catalytic C–H borylation reactions (Scheme 1).^{7–10} Despite their very high catalytic activity, high cost, and lower abundance of these rare metals in earth's crust raises concern over their use as catalysts, replacement by nonprecious, earth-abundant, nontoxic metal catalysts is thus considered as an alternative to such precious metals.¹¹ In 1995, Hartwig and co-workers demonstrated that the complex (Cp)Fe(CO)₂(Bcat) (Cp = cyclopentadienyl, cat = catecholate) can stoichiometrically transfer its catechol–borane part to borylate benzene under photochemical conditions.¹² Soon after this experimen-

Scheme 1. Overview of Transition-Metal-Catalyzed C(sp²)–H Borylation of Arenes

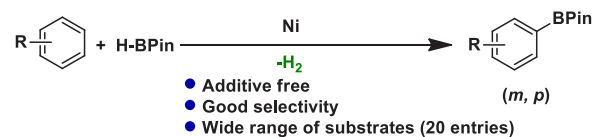
Traditional approach:



Nickel catalyzed approach:



Our approach:



tal discovery, a plethora of base-metal catalysts has come into the picture toward catalytic C–H borylation. In 2010, Kuang, Wang, and co-workers used γ -Fe₂O₃ nanoparticles toward arene borylation in presence of more than an equivalent amount of base and oxidant.¹³ Mankad et al. relied upon metal–metal cooperativity to accomplish this task by introducing various heterobimetallic systems under photochemical conditions.¹⁴ Darcel, Etienne, Sortais, Bontemps, and co-workers have introduced Fe(Me)₂(dmpe)₂ (dmpe = 1,2-bis(dimethylphosphino)ethane) for borylation of arenes with the help of UV irradiation.¹⁵ All of these methods involving base-metal catalysts still suffered from major drawbacks such as versatility in substrate scope, use of excess base, oxidant, H₂

Received: May 31, 2019

acceptor, and photochemical setup involving UV or Hg lamp. Chirik and co-workers further attempted to address such drawbacks by activating arenes under thermal conditions. In 2014, Chirik et al. first demonstrated a series of highly active cobalt complexes bearing pincer ligands which can borylate arenes with only 1 mol % loading of catalyst under thermal conditions.¹⁶ Later on, the underlying mechanism was explained in detail¹⁷ to demonstrate the site-selective borylation of fluoroarenes in presence of fluorine as an ortho-directing group.¹⁸

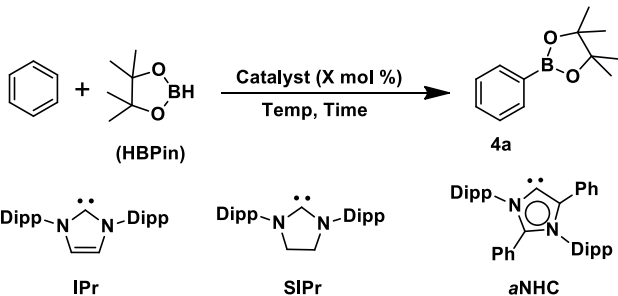
However, borylation of more challenging long branched alkyl chain substituted arenes was not addressed in such studies. In parallel efforts, Chatani et al. and Itami et al. have demonstrated nickel-catalyzed C(sp²)-H borylation of arenes and heteroarenes.^{19,20} Chatani and co-workers introduced an N-heterocyclic carbene (NHC) salt with a catalytic amount of Ni(COD)₂ (COD = 1,5-cyclooctadiene) and base to accomplish the borylation of arenes under thermal conditions using pinacolborane (HBPin).¹⁹ However, such a methodology has a very limited scope of arenes (only four examples), as it suffers from the selectivity of C(sp²)-H borylation over C(sp³)-H for substituted arenes (Scheme 1). On the other hand, Itami and co-workers used a phosphine-based ligand in combination with Ni(COD)₂ in presence of cesium fluoride and excess of arene (>50 equiv) to obtain the desired product at very high temperature (140 °C).²⁰ Once again, this report documents only three arenes, raising concern over the general applicability of this method.

Despite all these advances, the major limitation using base-metal catalysts without photochemical stimulation lies in the fact that they cannot borylate a wide range of arene substrates using HBPin. Furthermore, this field has not yet fully explored the scope of the nickel catalyst. It may be worth mentioning that Chatani et al. as well as Itami et al. in two independent studies earlier suggested that the nickel-catalyzed borylation reaction does not follow the conventional pathway reported earlier for iridium-,^{21,22} cobalt-,¹⁷ and iron-catalyzed¹⁵ processes; rather, it might follow a heterogeneous pathway. The reports both suggested formation of black particles during the catalysis and concluded that more detailed study is needed to get insights into the nature of these black particles. In this study, we report the first well-defined abnormal N-heterocyclic carbene, a 1,3-bis(2,6-diisopropylphenyl)-2,4-diphenylimidazol-5-ylidene (*a*NHC)-based nickel catalyst, for borylation of C(sp²)-H bonds for a wide variety of arenes. During the catalytic reaction, we also observed formation of black particles, which we have characterized as nickel(0) nanoparticles (Ni-NPs).

RESULTS AND DISCUSSION

The present study was initiated with optimization of reaction conditions for the direct C-H borylation of benzene using 4,4,5,5-tetramethyl-1,3,2-dioxaborolane (HBPin), Ni(COD)₂, and abnormal N-heterocyclic carbene (*a*NHC). Various reaction conditions were examined by altering time, solvent, catalyst loading, and temperature, and in each case, formation of the desired product was observed but with varied efficiency (Table 1). The borylated product was obtained in negligible yield (<5%) with 1 mol % loading of Ni(COD)₂ and *a*NHC catalyst combination in 16 h at 80 °C (Table 1, entry 1). When the Ni(COD)₂ and *a*NHC loadings were increased to 2.5 mol % and all other parameters kept unchanged, the yield was significantly increased to 60% (Table 1, entry 2), and a further

Table 1. Optimization of Nickel-Catalyzed C-H Borylation^a



entry	catalyst (mol %)	time (h)	temp (°C)	yield (%) ^b
1	Ni(COD) ₂ / <i>a</i> NHC (1)	16	80	<5
2	Ni(COD) ₂ / <i>a</i> NHC (2.5)	16	80	60
3	Ni(COD) ₂ / <i>a</i> NHC (5)	12	80	74
4	Ni(COD) ₂ / <i>a</i> NHC (5)	16	80	85
5	Ni(COD) ₂ / <i>a</i> NHC (5)	16	room temp	0
6	Ni(COD) ₂ (5)	16	80	0
7	<i>a</i> NHC (5)	16	80	0
8	Ni(COD) ₂ /IPr (5)	16	80	14
9	Ni(COD) ₂ /SIPr (5)	16	80	17
10	1 (5)	16	80	88
11	2 (5)	16	80	44
12	1 (2.5)	16	80	55
13	1 (1)	16	80	<5

^aAll reactions were conducted with HBPin (0.5 mmol) and benzene (7.5 mmol) under neat conditions. ^bIsolated yield based on HBPin.

increment in yield (74%) was found when a 5 mol % of Ni(COD)₂ and *a*NHC catalyst combination was used (Table 1, entry 3). Delightfully, the yield was further improved to 85% on elongating the time period to 16 h (Table 1, entry 4). The reaction did not proceed at room temperature (Table 1, entry 5). Reaction with either Ni(COD)₂ or *a*NHC did not result in any product formation, authenticating the indispensable role of an active catalyst in this reaction (Table 1, entries 6 and 7). Next, we examined two other normal N-heterocyclic carbenes (IPr and SIPr) in combination with Ni(COD)₂. In both cases, the desired product was formed in very low yield, 14–17% (Table 1, entries 8 and 9). It may be concluded from the above observations that the abnormal N-heterocyclic carbene (*a*NHC) has a better catalytic activity than the normal N-heterocyclic carbene (NHC) in association with Ni(COD)₂. The theoretically calculated energies for HOMO and HOMO-1 orbitals for *a*NHC (−4.403 and −4.879 eV, respectively) are much higher than that of the normal isomeric NHC (−5.000 and −5.279 eV, respectively), which makes *a*NHC more nucleophilic than its normal analogue.²³

Next, we prepared the two nickel catalysts **1** and **2** (Figure 1a) through modification of the reported procedure by using 1,3-bis(2,6-diisopropylphenyl)-2,5-diphenyl-1*H*-imidazol-3-ium chloride hydrochloride (**L1**) or 1,3-bis(2,6-diisopropylphenyl)-5-(4-methoxyphenyl)-2-phenyl-1*H*-imidazol-3-ium chloride hydrochloride (**L2**) instead of the corresponding free carbene.²⁴ The syntheses of **1** and **2** were accomplished by reacting Ni(COD)₂ with **L1** and **L2** in the presence of a base, potassium bis(trimethylsilyl)amide (KHMDS), in a 1:1:2.1 stoichiometric ratio.

The addition of dry THF to this mixture at −78 °C under an N₂ atmosphere resulted in a sharp color change from pale yellow to dark red with the formation of complex **1** or **2**

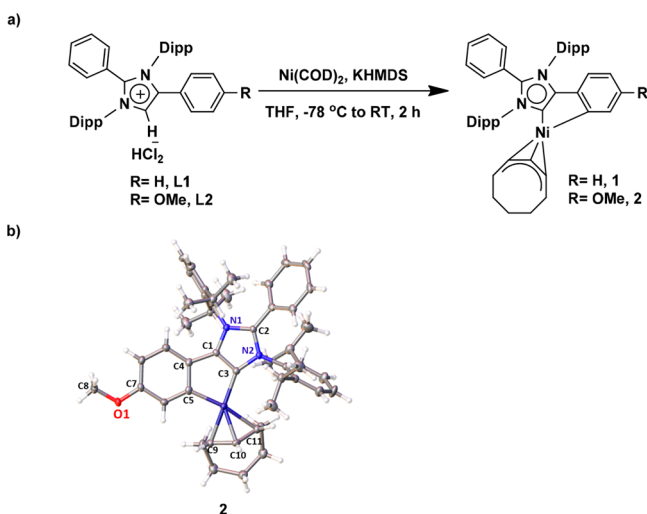


Figure 1. (a) Syntheses of *a*NHC-based nickel complexes. (b) Molecular structure of **2**. Thermal ellipsoids represent 50% probability; residual solvent molecules and disordered atoms are omitted for the sake of clarity. Selected bond distances (Å) and angles (deg) are as follows: Ni1–C3 1.907(2), Ni1–C5 1.954(2), Ni1–C9 2.022(2), Ni1–C10 1.965(2), Ni1–C11 2.101(2); C3–Ni1–C5 84.66(9), C3–Ni1–C9 172.54(9), C9–Ni1–C11 73.76(9), and C10–Ni1–C9 41.42(9).

(Figure 1a). Analytically pure crystals were obtained from a toluene/hexane mixture at 15 °C after 3 days. Complex **1** was characterized by ^1H and ^{13}C NMR spectroscopy, and these data matched with the literature data.²⁴ Complex **2** was characterized by an array of spectroscopic tools (^1H and ^{13}C NMR spectroscopy) as well as elemental analysis and single-crystal X-ray diffraction studies. The molecular structure of **2** is shown in Figure 1b.

Complexes **1** and **2** were tested for their catalytic activity. The reaction proceeded smoothly with catalyst **1**, affording

88% yield (Table 1, entry 10). A further decrease in mole percent of **1** did not give any satisfactory yield (Table 1, entries 12 and 13). However, introduction of **2** resulted in low yield (44%, Table 1, entry 11). This observation may be explained by considering a previous report²⁵ which documents that the carbene generated from **L2** is less stable than that generated from **L1**. It may be possible that, during the metathesis step, it is quenched before formation of the analogue of compound **3** (Figure 2a) and ends up with a smaller yield. These observations encouraged us to take forward this borylation reaction with catalyst **1** to explore further the scope of the reaction. To increase the scope of boranes, we have also introduced $\text{B}_2\text{Pin}_2/9\text{-BBN}$ as a borane source but no product formation was observed under our standard protocol for this borylation reaction. A 69:31 selectivity of meta- and para-substituted products was obtained in the case of toluene. It is worth mentioning that borylation of toluene, ethylbenzene, or any alkyl benzene took place selectively at the $\text{C}(\text{sp}^2)\text{-H}$ position instead of the benzylic position¹⁹ (Scheme 2, **4b–m,p,q**), resulting in moderate to excellent yield (57–83%). Furthermore, a meta-borylated product was obtained as the major species, which is consistent with the previously reported iridium catalysts.^{26,27} Next, xylene derivatives were borylated in very good yield (68–70%, Scheme 2, **4k,l**). The most difficult substrate among xylenes, *p*-xylene resulted in moderate yield (54%, Scheme 2, **4m**). In case of *m*-xylene, a very good selectivity was noted, as only a single borylated product at the C5-position of the phenyl ring was obtained. The borylation of a solid substrate was carried out: for example, naphthalene is considered to be one of the most challenging substrates to borylate through a direct C–H bond. Even iridium-catalyzed borylation of naphthalene resulted in diborylated products in major amount.²⁸ Delightfully, the present reaction conditions resulted selectively in monoborylated naphthalene in 61% isolated yield with high β/α selectivity (86:14, Scheme 2, **4o**). Another solid substrate, biphenyl, can also be borylated in

Use the following as Figure 2.

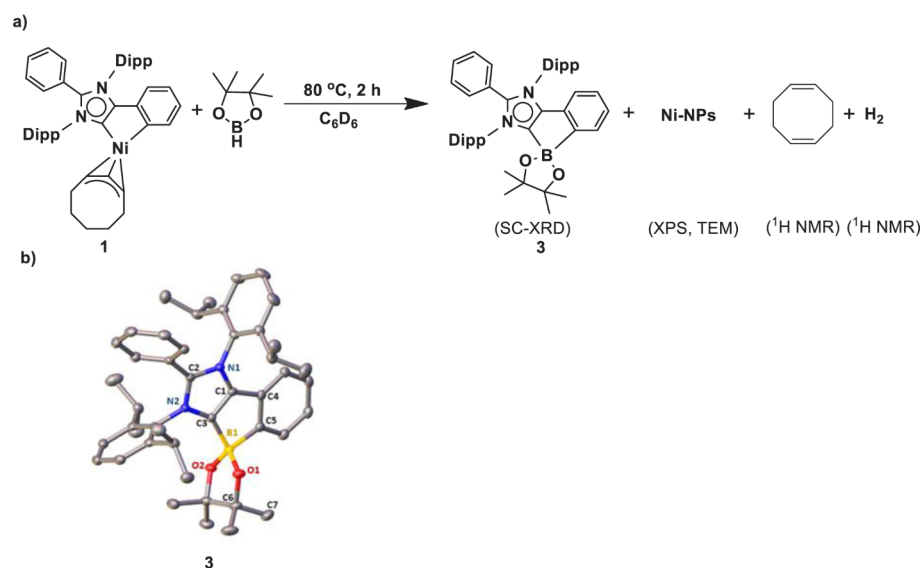
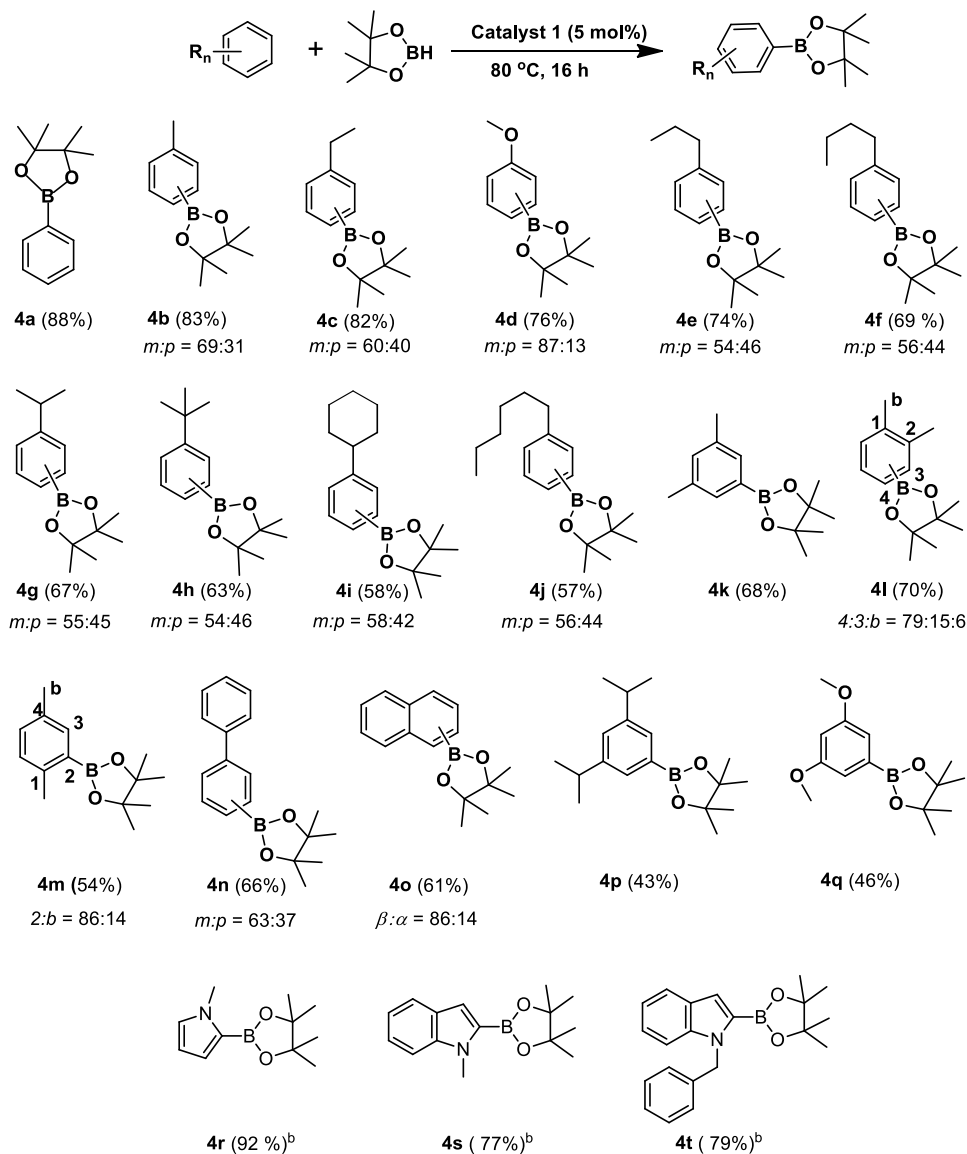


Figure 2. (a) Synthesis of compound **3**. (b) Molecular structure of **3**. Thermal ellipsoids represent 50% probability; hydrogen atoms and residual solvent molecules are omitted for the sake of clarity. Selected bond distances (Å) and angles (deg) are as follows: C3–B1 1.6920(17), C5–B1 1.6738(18), O1–B1 1.4717(16), O2–B1 1.4569(16), O1–B1–O2 106.24(10), O1–B1–C5 114.04(10), O2–B1–C3 120.71(10), and C5–B1–C3 93.80(9).

Scheme 2. Reaction Scope for Nickel-Catalyzed C–H Borylation of Arenes^a

^aAll reactions were conducted with HBPIn (0.5 mmol) and arene (7.5 mmol). The isolated yield based on HBPIn is given in parentheses. Product ratios were determined via NMR spectroscopy analysis. Conditions: **4c,e–o**, 100 °C for 24 h; **4p,q**, 100 °C for 24 h, 7.5 mol % catalyst was used. ^bConditions: heteroarene (0.5 mmol), HBPIn (0.75 mmol), catalyst (0.025 mmol), 80 °C, 16 h, methylcyclohexane as solvent. For **4r–t**, isolated yields are based on heteroarene.

good yield under our reaction conditions (66%, Scheme 2, **4n**). Furthermore, it was noted that even an arene bearing sterically bulky groups such as isopropyl, *tert*-butyl, and cyclohexyl resulted in such borylation successfully with impressive yield (58–67%, Scheme 2, **4g–i**). A similar finding was also observed for the borylation of *n*-propyl-, *n*-butyl-, and *n*-hexylbenzene (57–74%, Scheme 2, **4e,f,j**). The *m:p* selectivities are also consistent with the previously reported iridium(0) nanoparticle catalyzed borylation of arenes.¹⁰ This result encouraged us to check whether more sterically hindered arenes can undergo C(sp²)-H borylation under the optimized conditions. Borylation of 1,3-diisopropylbenzene and 1,3-dimethoxybenzene led to the formation of single isomer selectively (Scheme 2, **4p,q**), however, with relatively low yields of 43% and 46%, respectively. This result is consistent with earlier results reporting borylation at the most sterically accessible C–H bonds (C5-position of the phenyl ring).⁷ Next,

we examined whether heteroarenes such as pyrrole and indole can be borylated using our protocol. *N*-Methylpyrrole was borylated successfully at the C-2 position with excellent yield (92%, Scheme 2, **4r**). *N*-Methylindole and *N*-benzylindole also resulted in the formation of C-2 borylated products in good yield (77–79%, Scheme 2, **4s,t**), which may be compared with a previous report leading to single isomeric borylated products for heteroarenes.¹⁹ To the best of our knowledge, earlier studies never addressed direct C(sp²)-H borylation of *n*-hexylbenzene, *n*-butylbenzene, *n*-propylbenzene, phenylcyclohexane, naphthalene, biphenyl, 1,3-diisopropylbenzene, and 1,3-dimethoxybenzene using first-row transition-metal catalysts.

Having the optimized reaction conditions in hand, we continued to explore the borylation of different arenes under neat conditions. Borylation of benzene and toluene proceeded

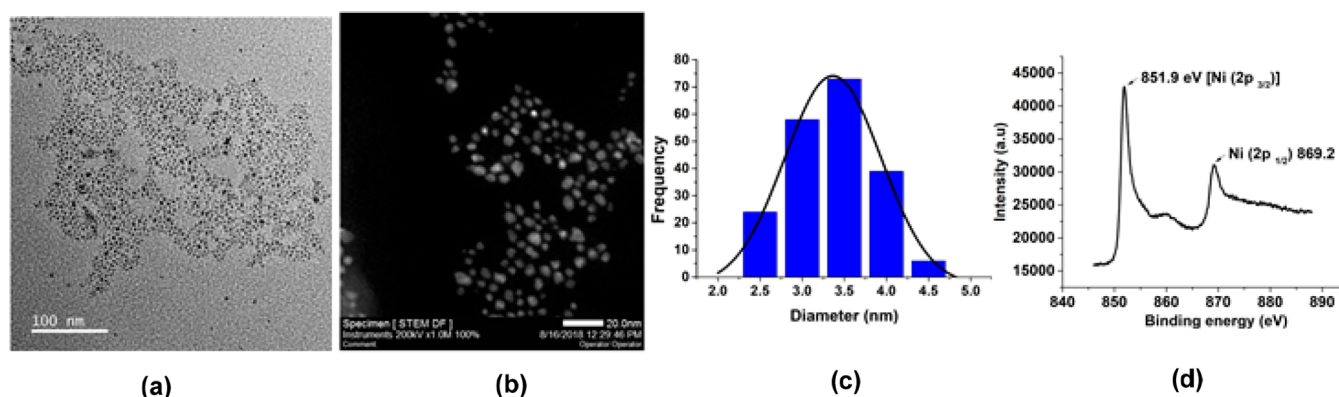


Figure 3. (a) TEM image of the Ni-NPs obtained from a 1:1 reaction mixture of **1** and HBPIn. (b) STEM image of Ni-NPs. (c) Histogram of the Ni-NPs size distribution (average diameter $3.4(\pm 0.5)$ nm), constructed from the measurement of 200 NPs. (d) XPS spectrum of Ni-NPs.

smoothly, affording 88% and 83% yields, respectively (Scheme 2, **4a,b**).

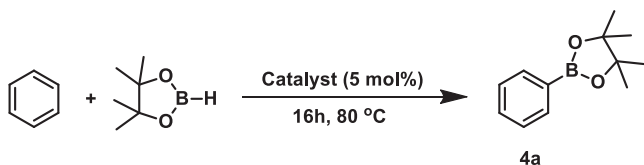
While performing the catalytic reactions, we noticed that there was deposition of black particles on the wall of the reaction vessel. This is reminiscent of the earlier observation reported by Chatani and Itami et al. in two independent studies during nickel-catalyzed C(sp²)-H borylation reactions.^{19,20} However, these studies did not provide any further details on such black particle formation. Next, we performed the catalytic borylation reaction in the presence of mercury (10 equiv with respect to **1**).¹⁹ The addition of mercury completely arrested the reaction, as one might expect in the case of a heterogeneous reaction. A kinetic isotope experiment was carried out with equimolar amounts of benzene and benzene-*d*₆, and the $k_{\text{H}}/k_{\text{D}}$ value was measured as 1.76 (see Figure S70 in the Supporting Information), which is comparable to that reported (1.99) earlier, indicating that breaking of a C-H bond may be involved in the rate-determining step.^{19,20} To gather further information, a series of stoichiometric reactions was performed. First, a stoichiometric mixture of HBPIn and **1** in C₆D₆ was heated at 80 °C for 2 h over a hot plate under closed conditions (Figure 2a). The mixture was cooled down to room temperature and kept for crystallization after adding hexane. Within 10 h, appearance of yellowish crystals was observed along with a black precipitate. One of these crystals was analyzed by a single-crystal X-ray diffractometer.

The molecular structure of **3** (Figure 2b) revealed the formation of an unprecedented compound in which the Ni(II) ion was replaced by the B(III) ion to form the tetrahedrally coordinated boron compound **3** (Figure 2a). The crystals of **3** were found to be highly air and moisture sensitive, and it immediately decomposes on exposure to air. Additionally, to support the findings, we noted that, on addition of HBPIn to **1**, gas evolution was observed, which was characterized as H₂ by ¹H NMR spectroscopy (δ 4.57 in CD₃CN).²⁹ Attempts to get more information about the intermediates in the course of formation of **3** were unsuccessful. We performed an ¹¹B NMR spectroscopy study by adding a stoichiometric amount of HBPIn to a C₆D₆ solution of **1**. However, within 15 min of addition of HBPIn to the solution of **1**, the formation of **3** was detected through ¹¹B NMR spectroscopic experiment (see Figure S68 in the Supporting Information). After 2 h of heating at 80 °C, HBPIn was fully consumed and the peak due to **3** became prominent (see Figure S69 in the Supporting Information). The formation of free 1,5-cyclooctadiene was also authenticated as a side product along with H₂ by ¹H NMR

spectroscopy (δ 2.21 (m, 8H), 5.57 (m, 4H) ppm) from the reaction mixture in C₆D₆.³⁰ Furthermore, we observed the formation of black particles during the course of the reaction, which have been characterized as Ni-NPs by transmission electron microscopy (TEM) and X-ray photoelectron spectroscopic (XPS) measurements (Figure 3). The formation of Ni-NPs is similar to that reported for reduction of Ni(II) salts or by decomposition of Ni(COD)₂ in ionic liquids.^{31,32} Furthermore, transmission electron microscopy (TEM) of the black particles displayed spherical metallic nanoparticles distributed uniformly (Figure 3a). The scanning transmission electron microscopic (STEM) images displayed a clear picture of the shape and size of Ni-NPs (Figure 3b). The TEM images unveiled a highly monodisperse nature of the nickel nanoparticles of average diameter $3.4(\pm 0.5)$ nm (Figure 3a,c). In addition, an X-ray photoelectron spectroscopic (XPS) measurement was performed to gain more insight on the oxidation state of nickel which revealed Ni 2p_{3/2,1/2} peaks at 851.9 and 869.2 eV, confirming the formation of metallic nickel (Figure 3d).³³ The formation of Ni-NPs along with compound **3** in the course of C-H borylation of arenes was well-characterized using several spectroscopic techniques (¹H, ¹³C, ¹¹B NMR spectroscopy, TEM, XPS) and an X-ray crystallographic study.

A series of control experiments was carried out to check the catalytic activity of Ni-NPs. At first, we prepared nickel nanoparticles (Ni-NPs) from another Ni precursor such as Ni(COD)₂ in the presence of a stoichiometric amount of HBPIn (black mass deposition) on heating at 80 °C for 2 h, but failed to accomplish the catalytic borylation reaction of benzene. Next, Ni-NPs were isolated from the stoichiometric reaction of **1** and HBPIn. However, a trace amount of product was realized using only Ni-NPs (Table 2, entry 1). Alternatively, the catalytic activity was tested using compound **3**, which did not result in the formation of the desired product (Table 2, entry 2). However, an excellent yield was achieved when a mixture of Ni-NPs and **3** was introduced (Table 2, entry 3). When all these results are combined, it may be concluded that the presence of a heterogeneous mixture of Ni-NPs and **3** is needed to proceed with the catalysis.

This reaction follows a heterogeneous pathway where Ni-NPs in the presence of compound **3** form the catalytically active species. The mechanism of the reaction may be proposed on the basis of the previously reported iridium nanoparticle catalyzed borylation of arenes^{10,34,35} following activation of either an arene C-H bond to produce reactive

Table 2. Controlled Experiments^a

entry	catalyst	yield ^b
1	Ni-NPs	<5%
2	3	0
3	Ni-NPs and 3	83%

^aBenzene (3.75 mmol), HBPIn (0.25 mmol). ^bIsolated yield based on HBPIn.

Ni–Ar or Ni–H species or reaction with HBPIn to produce Ni–H and Ni–BPIn species. This reductive elimination may result in the formation of the product and generates the active catalyst with the simultaneous liberation of H₂ gas.

In conclusion, this report documents catalytic C(sp²)–H borylation of a wide variety of arenes using a nickel catalyst. For the first time, we could perform borylation of *n*-hexylbenzene, *n*-butylbenzene, *n*-propylbenzene, phenylcyclohexane, naphthalene, biphenyl, 1,3-diisopropylbenzene, and 1,3-dimethoxybenzene using a first row transition metal catalyzed direct C(sp²)–H borylation reaction. Mono- and disubstituted alkyl and alkoxy arenes as well as solid substrates can also be borylated under these reaction conditions. Active reaction intermediates were also characterized by an array of spectroscopic and microscopic studies as well as X-ray crystallographic studies.

EXPERIMENTAL SECTION

General Considerations. All air- and moisture-sensitive manipulations were carried out using standard high-vacuum-line, Schlenk, or cannula techniques or in an MBraun drybox containing an atmosphere of purified nitrogen. Glasswares were dried overnight at 130 °C before use. All solvents and arenes were dried over a Na/benzophenone mixture and distilled under inert conditions before use. The ¹H and ¹³C NMR spectra were recorded on 400 and 500 MHz NMR spectrometers with residual undeuterated solvent as an internal standard. ¹¹B NMR spectra were obtained by using a Bruker Avance 500 MHz NMR spectrometer. Chemical shifts for ¹¹B NMR spectra were referenced using Et₂O·BF₃ as an external standard. Chemical shifts (δ) are given in ppm, and J values are given in Hz. For transmission electron microscopy (TEM) imaging, Ni-NPs were dispersed in hexane by ultrasonication to obtain a stable dispersion of the particles. One drop of this solution was drop-cast onto the carbon-coated Cu-based grid (Ted Pella, Inc., 300 mesh Cu), and TEM images were recorded with JEOL apparatus, Model JEM-2100F. TEM images in STEM (HAADF) mode were taken at the UHR-FEG-TEM, DST-FIST facility of IISER Kolkata. For X-ray photoelectron spectroscopy (XPS) experiments, Ni-NPs were dispersed in hexane by sonication and 10–15 drops of solution were drop-cast onto a glass plate (area <1 cm²). Solvent was fully dried under vacuum, and the experiment was conducted on an Omicron Nano Technology (Model 0571) XPS spectrometer using an aluminum anode (Al Kα, 1486.6 eV) run at 15 kV and 10 mA as an X-ray source.

General Procedure for Borylation of Arenes. In a nitrogen-filled glovebox, a 15 mL sealed tube equipped with a Teflon-sealed screw cap was charged with a magnetic bar, nickel complex **1** (17.7 mg, 0.025 mmol), 4,4,5,5-tetramethyl-1,3,2-dioxaborolane (HBPIn, 72 μL, 0.5 mmol), and the corresponding arene (7.5 mmol). Subsequently, the mixture was heated to 80 or 100 °C for 16–24 h. After completion of the reaction, the reaction mixture was diluted with 50 mL of an ethyl acetate and hexane (1/5) solvent mixture. It

was then passed through a pad of Celite. Solvent was evaporated under reduced pressure using a rotary evaporator. Borylated products were isolated through a silica column (100–200 mesh) using an ethyl acetate and hexane mixture.

General Procedure for Borylation of Heteroarenes. In a nitrogen-filled glovebox, **1** (0.025 mmol), HBPin (0.75 mmol), the appropriate heteroarene (0.5 mmol), and dry methylcyclohexane were added together in a 15 mL sealed tube equipped with a Teflon-sealed screw cap. Next, the mixture was heated at 80 °C for 16 h. After completion of the reaction, the reaction mixture was diluted with 50 mL of an ethyl acetate and hexane (1/5) mixture. It was then passed through a pad of Celite. Solvent was evaporated under reduced pressure using a rotary evaporator. Borylated products were isolated through a silica (100–200 mesh) column using an ethyl acetate and hexane mixture.

Hg Drop Test.¹⁹ Inside a N₂-filled glovebox, **1** (17.7 mg, 0.025 mmol), HBPin (72 μL, 0.5 mmol), and Hg (55 mg, 0.275 mmol) were placed in a 15 mL sealed tube containing 1 mL of benzene. The sealed tube was tightly sealed with a screw cap and heated to 80 °C for 16 h with stirring over a hot plate. The resulting mixture was diluted with 20 mL of an ethyl acetate and hexane (1/5) mixture to pass it through a bed of silica, and solvent was fully removed under vacuum. The formation of the desired borylated product was not observed by proton NMR spectroscopy.

Preparation of **1 and **2**.** A 50 mL Schlenk flask was charged with 1,3-bis(2,6-diisopropylphenyl)-2,5-diphenyl-1*H*-imidazol-3-ium chloride hydrochloride and **L1** (613 mg, 1.0 mmol) and kept under vacuum for 2 h at 80 °C. Next, it was transferred to a nitrogen-filled glovebox to add Ni(COD)₂ (275 mg, 1.0 mmol) and potassium bis(trimethylsilyl)amide (419 mg, 2.1 mmol). It was taken out of the glovebox and 15 mL of dry THF was added through a cannula under a nitrogen atmosphere at –78 °C. The mixture was stirred for 2 h at room temperature. In this process, the color changed from pale yellow to dark red. The reaction mixture was fully dried under vacuum, and the complex was extracted in dry benzene. Analytically pure dark yellow crystals of **1** were obtained by recrystallization from benzene/hexane (1/7 v/v) mixture at 25 °C after 3 days. ¹H and ¹³C NMR spectra were recorded and matched with the literature data:²⁴ 568.4 mg, yield 80%.

The preparation of **2** was accomplished using 1,3-bis(2,6-diisopropylphenyl)-5-(4-methoxyphenyl)-2-phenyl-1*H*-imidazol-3-ium chloride hydrochloride, **L2** (322 mg, 0.5 mmol), Ni(COD)₂ (137.5 mg, 0.5 mmol), and potassium bis(trimethylsilyl)amide (220 mg, 1.1 mmol) following a procedure similar to that described for **1**. **2** was characterized by single-crystal X-ray crystallography and ¹H NMR and ¹³C NMR spectroscopic measurements: 280.5 mg, yield 76%. Anal. Calcd for C₅₄H₆₄N₂NiO: C, 79.50; H, 7.91; N, 3.43. Found: C, 79.34; H, 8.10; N, 3.73.

Complex **2.** ¹H NMR (400 MHz, C₆D₆, 298 K): δ (ppm) 8.10 (d, J = 7.2 Hz, 1H), 7.31–7.20 (m, 3H), 7.17 (s, 1H), 7.05 (d, J = 7.6 Hz, 1H), 6.98 (dd, J = 6.8 Hz, 3.2 Hz, 3H), 6.59 (m, 3H), 6.30 (dd, J = 8.4 Hz, 2.4 Hz, 1H), 6.03 (d, J = 8.4 Hz, 1H), 5.16 (t, J = 8.0 Hz, 1H), 4.01 (q, J = 8.4 Hz, 1H), 3.65 (quin, J = 7.2 Hz, 1H), 3.54 (s, 3H), 3.26 (q, J = 6.8 Hz, 1H), 3.19 (q, J = 6.8 Hz, 1H), 3.05 (quin, J = 6.8 Hz, 1H), 2.77 (quin, J = 6.8 Hz, 1H), 2.64–2.57 (m, 1H), 2.33–2.24 (m, 1H), 2.14–2.10 (m, 1H), 2.00–1.92 (m, 1H), 1.61–1.54 (m, 2H), 1.41 (d, J = 6.8 Hz, 6H), 1.33 (d, J = 6.8 Hz, 3H), 1.27–1.23 (m, 1H), 1.13 (d, J = 6.8 Hz, 3H), 1.09 (t, J = 6.4 Hz, 6H), 0.94 (d, J = 6.8 Hz, 3H), 0.65 (J = 6.8 Hz, 3H), 0.62 (d, J = 6.8 Hz, 3H). ¹³C NMR (100 MHz, C₆D₆, 298 K): δ (ppm) 172.8 (Ni–C_{Ar}), 168.8 (Ni–C_{Carbene}), 157.7, 151.0, 145.3, 144.4, 144.3, 143.0, 137.8, 137.2, 136.5, 132.0, 129.9, 128.9, 128.4, 127.5, 127.1, 126.9, 124.5, 124.3, 124.1, 123.7, 123.6, 117.8, 107.9, 106.0, 68.3, 63.3, 53.6, 32.1, 31.0, 29.0, 28.2, 28.1, 28.0, 27.9, 24.0, 23.2, 23.1, 22.4, 22.3, 22.2, 22.0, 21.5.

Preparation of **3.** Inside a N₂-filled glovebox, a 15 mL J. Young pressure tube equipped with a PTFE screw cap was charged with 50 mg of complex **1** (0.07 mmol) and it was dissolved in a minimum amount of dry benzene-*d*₆ (1.5 mL), resulting in a bright red solution. Next, 10.3 μL of 4,4,5,5-tetramethyl-1,3,2-dioxaborolane (HBPIn,

0.07 mmol) was placed in the vial. The mixture slowly turned into dark red from bright red. The tube was capped tightly and taken out of the glovebox to stir the mixture at 80 °C for 2 h under closed conditions. The mixture was cooled to room temperature and taken inside a glovebox. The black particles had already settled down at the bottom of the tube. The supernatant liquid was gently decanted to one 5 mL vial. Dry hexane (2.5 mL) was added carefully to make separate layers (1:1.7 v/v). These layers were kept for crystallization at room temperature after adding hexane (1.5 mL). After 10 h, good-quality yellowish block-shaped crystals were found to grow inside the vial: 20.8 mg, yield 44%. Due to high air and moisture sensitivity, the elemental analysis experiment of 3 was unsuccessful. ¹H NMR (400 MHz, C₆D₆, 298 K): δ (ppm) 8.15 (d, *J* = 6.8 Hz, 1H), 7.25–7.19 (m, 2H), 7.12 (d, *J* = 7.6 Hz, 3H), 7.01–6.97 (m, 4H), 6.84 (t, *J* = 7.2 Hz, 1H), 6.55–6.53 (m, 3H), 6.17 (d, *J* = 7.2 Hz, 1H), 3.33 (quin, *J* = 6.4 Hz, 1H), 2.84 (quin, *J* = 6.4 Hz, 1H), 1.67 (d, *J* = 6.4 Hz, 6H), 1.62 (s, 6H), 0.96 (s, 6H), 0.87 (t, *J* = 7.2 Hz, 12H), 0.81 (d, *J* = 6.4 Hz, 6H). ¹³C NMR (100 MHz, C₆D₆, 298 K): δ (ppm) 148.0, 145.8, 145.2, 142.2, 135.5, 135.2, 132.7, 132.1, 131.4, 130.6, 128.9, 128.4, 125.3, 125.2, 124.9, 124.3, 117.4, 78.8, 29.1, 27.7, 26.2, 24.7, 24.2, 23.1, 22.8. ¹¹B NMR (160 MHz, C₆D₆, 298 K): δ (ppm) 8.0.

H₂ Evolution Experiment. Inside a N₂-filled glovebox, a 2.5 mL screw cap NMR tube was charged with **1** (15 mg, 0.021 mmol) and acetonitrile-*d*₃ (0.6 mL). HBPIn (4.1 μL, 0.028 mmol) was next added, and immediately the Teflon screw cap was placed tightly. As soon as the HBPIn was added to the CD₃CN solution of **1**, gas evolution was noticed which was confirmed as dihydrogen from an ¹H NMR (δ 4.57 ppm in CD₃CN) spectrum (Figure S66).³⁰

1,5-Cyclooctadiene Liberation Experiment. Inside a N₂-filled glovebox, a 2.5 mL screw cap NMR tube was charged with **1** (10 mg, 0.014 mmol), and it was dissolved in 0.6 mL of C₆D₆. HBPIn (10.1 μL, 0.07 mmol) was next added, and immediately the Teflon cap was tightly placed. The ¹H NMR spectrum revealed two significant peaks of 1,5-cyclooctadiene at δ 2.21 (m, 8H), 5.57 (m, 4H) ppm (Figure S67). The peak values matched with the reported literature.³²

k_H/k_D Experiment. A 15 mL sealed tube was charged with a magnetic bar and 17.7 mg (0.025 mmol) of **1**, 72 μL (0.5 mmol) of HBPIn, and 670 μL (7.5 mmol) of both benzene and benzene-*d*₆. The tube was then carefully capped using a Teflon-sealed screw cap and placed at 80 °C for 16 h. After completion of the reaction, the reaction mixture was quenched with 50 mL of an ethyl acetate/hexane mixture (1/5) and passed through a pad of Celite. Solvent was removed under vacuum. The k_H/k_D value was determined by the ratio of products obtained using an ¹H NMR spectroscopic experiment (Figure S70).^{19,20}

■ ASSOCIATED CONTENT

Supporting Information

The Supporting Information is available free of charge on the ACS Publications website at DOI: 10.1021/acs.organomet.9b00364.

Experimental details, spectral data, and ¹H, ¹³C, and ¹¹B NMR spectra (PDF)

Accession Codes

CCDC 1890848–1890849 contain the supplementary crystallographic data for this paper. These data can be obtained free of charge via www.ccdc.cam.ac.uk/data_request/cif, or by emailing data_request@ccdc.cam.ac.uk, or by contacting The Cambridge Crystallographic Data Centre, 12 Union Road, Cambridge CB2 1EZ, UK; fax: +44 1223 336033.

■ AUTHOR INFORMATION

Corresponding Author

*E-mail for S.K.M.: swadhin.mandal@iiserkol.ac.in.

ORCID

Swadhin K. Mandal: 0000-0003-3471-7053

Notes

The authors declare no competing financial interest.

■ ACKNOWLEDGMENTS

We thank the SERB (DST) of India (Grant No. EMR/2017/000772). A.D. and P.K.H. thank the IISER Kolkata for research fellowships. A.D. thanks Sourav Ghosh, IISER-Kolkata, for his help in TEM and XPS studies. The authors also thank the NMR, X-ray, and TEM facilities of IISER-Kolkata.

■ REFERENCES

- (1) Campeau, L. C.; Chen, Q.; Gauvreau, D.; Girardin, M.; Belyk, K.; Maligres, P.; Zhou, G.; Gu, C.; Zhang, W.; Tan, L.; O'Shea, P. D. A Robust Kilo-Scale Synthesis of Doravirine. *Org. Process Res. Dev.* **2016**, *20*, 1476–1481.
- (2) Liao, X.; Stanley, L. M.; Hartwig, J. F. Enantioselective Total Syntheses of (–)-Taiwaniaquinone H and (–)-Taiwaniaquinol B by Iridium-Catalyzed Borylation and Palladium-Catalyzed Asymmetric R-Arylation. *J. Am. Chem. Soc.* **2011**, *133*, 2088–2091.
- (3) Ren, Y.; Sezen, M.; Guo, F.; Jakle, F.; Loo, Y. L. [*d*]-Carbon–Carbon Double Bond Engineering in Diazaphosphines: A Pathway to Modulate the Chemical and Electronic Structures of Heteropines. *Chem. Sci.* **2016**, *7*, 4211–4219.
- (4) Mkhaliid, I. A. I.; Barnard, J. H.; Marder, T. B.; Murphy, J. M.; Hartwig, J. F. C–H Activation for the Construction of C–B Bonds. *Chem. Rev.* **2010**, *110*, 890–931.
- (5) Hartwig, J. F. Borylation and Silylation of C–H Bonds: A Platform for Diverse C–H Bond Functionalizations. *Acc. Chem. Res.* **2012**, *45*, 864–873.
- (6) Preshlock, S. M.; Ghaffari, B.; Maligres, P. E.; Krska, S. W.; Maleczka, R. E., Jr.; Smith, M. R., III High-Throughput Optimization of Ir-Catalyzed C–H Borylation: A Tutorial for Practical Applications. *J. Am. Chem. Soc.* **2013**, *135*, 7572–7582.
- (7) Bheeter, C. B.; Chowdhury, A. D.; Adam, R.; Jackstell, R.; Beller, M. Efficient Rh-Catalyzed C–H Borylation of Arene Derivatives Under Photochemical Conditions. *Org. Biomol. Chem.* **2015**, *13*, 10336–10340.
- (8) Furukawa, T.; Tobisu, M.; Chatani, N. C–H Functionalization at Sterically Congested Positions by the Platinum-Catalyzed Borylation of Arenes. *J. Am. Chem. Soc.* **2015**, *137*, 12211–12214.
- (9) Kawamorita, S.; Miyazaki, T.; Ohmiya, H.; Iwai, T.; Sawamura, M. Rh-Catalyzed Ortho-Selective C–H Borylation of N-Functionalized Arenes with Silica-Supported Bridgehead Monophosphine Ligands. *J. Am. Chem. Soc.* **2011**, *133*, 19310–19313.
- (10) Yinghuai, Z.; Chenyan, K.; Peng, A. T.; Emi, A.; Monalisa, W.; Louis, L. K. J.; Hosmane, N. S.; Maguire, J. A. Catalytic Phenylborylation Reaction by Iridium(0) Nanoparticles Produced from Hydrido-iridium Carborane. *Inorg. Chem.* **2008**, *47*, 5756–5761.
- (11) Semproni, S. P.; Milsman, C.; Chirik, P. J. Four-Coordinate Cobalt Pincer Complexes: Electronic Structure Studies and Ligand Modification by Homolytic and Heterolytic Pathways. *J. Am. Chem. Soc.* **2014**, *136*, 9211–9224.
- (12) Waltz, K. M.; He, X.; Muhoro, C.; Hartwig, J. F. Hydrocarbon Functionalization by Transition Metal Boryls. *J. Am. Chem. Soc.* **1995**, *117*, 11357–11358.
- (13) Yan, G.; Jiang, Y.; Kuang, C.; Wang, S.; Liu, H.; Zhang, Y.; Wang, J. Nano-Fe₂O₃-Catalyzed Direct Borylation of Arenes. *Chem. Commun.* **2010**, *46*, 3170–3172.
- (14) Mazzacano, T. J.; Mankad, N. P. Base Metal Catalysts for Photochemical C–H Borylation That Utilize Metal–Metal Cooperativity. *J. Am. Chem. Soc.* **2013**, *135*, 17258–17261.
- (15) Dombay, T.; Werncke, C. G.; Jiang, S.; Grellier, M.; Vendier, L.; Bontemps, S.; Sortais, J. B.; Etienne, S. S.; Darcel, C. Iron-Catalyzed C–H Borylation of Arenes. *J. Am. Chem. Soc.* **2015**, *137*, 4062–4065.
- (16) Obligacion, J. V.; Semproni, S. P.; Chirik, P. J. Cobalt-Catalyzed C–H Borylation. *J. Am. Chem. Soc.* **2014**, *136*, 4133–4136.

- (17) Obligacion, J. V.; Semproni, S. P.; Pappas, I.; Chirik, P. J. Cobalt-Catalyzed C(sp²)-H Borylation: Mechanistic Insights Inspire Catalyst Design. *J. Am. Chem. Soc.* **2016**, *138*, 10645–10653.
- (18) Obligacion, J. V.; Bezdek, M. J.; Chirik, P. J. C(sp²)-H Borylation of Fluorinated Arenes Using an Air-Stable Cobalt Precatalyst: Electronically Enhanced Site Selectivity Enables Synthetic Opportunities. *J. Am. Chem. Soc.* **2017**, *139*, 2825–2832.
- (19) Furukawa, T.; Tobisu, M.; Chatani, N. Nickel-Catalyzed Borylation of Arenes and Indoles via C–H Bond Cleavage. *Chem. Commun.* **2015**, *51*, 6508–6511.
- (20) Zhang, H.; Hagihara, S.; Itami, K. Aromatic C–H Borylation by Nickel Catalysis. *Chem. Lett.* **2015**, *44*, 779–781.
- (21) Tamura, H.; Yamazaki, H.; Sato, H.; Sakaki, S. Iridium-Catalyzed Borylation of Benzene with Diboron. Theoretical Elucidation of Catalytic Cycle Including Unusual Iridium(V) Intermediate. *J. Am. Chem. Soc.* **2003**, *125*, 16114–16126.
- (22) Boller, T. M.; Murphy, J. M.; Hapke, M.; Ishiyama, T.; Miyaura, N.; Hartwig, J. F. Mechanism of the Mild Functionalization of Arenes by Diboron Reagents Catalyzed by Iridium Complexes. Intermediacy and Chemistry of Bipyridine-Ligated Iridium Trisboryl Complexes. *J. Am. Chem. Soc.* **2005**, *127*, 14263–14278.
- (23) Aldeco-Perez, E.; Rosenthal, A. J.; Donnadieu, B.; Parameswaran, P.; Frenking, G.; Bertrand, G. Isolation of a C5-Deprotonated Imidazolium, a Crystalline “Abnormal” N-Heterocyclic Carbene. *Science* **2009**, *326*, 556–559.
- (24) Vijaykumar, G.; Jose, A.; Vardhanapu, P. K.; P, S.; Mandal, S. K. Abnormal-NHC-Supported Nickel Catalysts for Hydroheteroarylation of Vinylarenes. *Organometallics* **2017**, *36*, 4753–4758.
- (25) Ung, G.; Bertrand, G. Stability and Electronic Properties of Imidazole-Based Mesoionic Carbenes. *Chem. - Eur. J.* **2011**, *17*, 8269–8272.
- (26) Ishiyama, T.; Takagi, J.; Ishida, K.; Miyaura, N.; Anastasi, N. R.; Hartwig, J. F. Mild Iridium-Catalyzed Borylation of Arenes. High Turnover Numbers, Room Temperature Reactions, and Isolation of a Potential Intermediate. *J. Am. Chem. Soc.* **2002**, *124*, 390–391.
- (27) Boebel, T. A.; Hartwig, J. F. Iridium-Catalyzed Preparation of Silyboranes by Silane Borylation and Their Use in the Catalytic Borylation of Arenes. *Organometallics* **2008**, *27*, 6013–6019.
- (28) Coventry, D. N.; Batsanov, A. S.; Goeta, A. E.; Howard, J. A. K.; Marder, T. B.; Perutz, R. N. Selective Ir-Catalyzed Borylation of Polycyclic Aromatic Hydrocarbons: Structures of Naphthalene-2,6-bis(boronate), Pyrene-2,7-bis(boronate) and Perylene-2,5,8,11-tetra(boronate) Esters. *Chem. Commun.* **2005**, 2172–2174.
- (29) Fulmer, G. R.; Miller, A. J. M.; Sherden, N. H.; Gottlieb, H. E.; Nudelman, A.; Stoltz, B. M.; Bercaw, J. E.; Goldberg, K. I. NMR Chemical Shifts of Trace Impurities: Common Laboratory Solvents, Organics, and Gases in Deuterated Solvents Relevant to the Organometallic Chemist. *Organometallics* **2010**, *29*, 2176–2179.
- (30) Enachi, A.; Baabe, D.; Zaretske, M. K.; Schweyen, P.; Freytag, M.; Raeder, J.; Walter, M. D. [(NHC)CoR₂]: Pre-catalysts for Homogeneous Olefin and Alkyne Hydrogenation. *Chem. Commun.* **2018**, *54*, 13798–13801.
- (31) Alonso, F.; Calvino, J. J.; Osante, I.; Yus, M. A New Straightforward and Mild Preparation of Nickel(0) Nanoparticles. *Chem. Lett.* **2005**, *34*, 1262–1263.
- (32) Migowski, P.; Machado, G.; Texeira, S. R.; Alves, M. C. M.; Morais, J.; Traverse, A.; Dupont, J. Synthesis and Characterization of Nickel Nanoparticles Dispersed in Imidazolium Ionic Liquids. *Phys. Chem. Chem. Phys.* **2007**, *9*, 4814–4821.
- (33) Wang, J.; Zhao, Q.; Hou, H.; Wu, Y.; Yu, W.; Ji, X.; Shao, L. Nickel Nanoparticles Supported on Nitrogen-Doped Honeycomb-like Carbon Frameworks for Effective Methanol Oxidation. *RSC Adv.* **2017**, *7*, 14152–14158.
- (34) Verma, P. K.; Shegavi, M. L.; Bose, S. K.; Geetharani, K. A Nano-Catalytic Approach for C–B Bond Formation Reactions. *Org. Biomol. Chem.* **2018**, *16*, 857–873.
- (35) Zhu, Y.; Hui, S.; Jang, A.; Tham, Y. H.; Algin, O. B.; Maguire, J. A.; Hosmane, N. S. An Efficient and Recyclable Catalytic System Comprising Nano-Iridium(0) and a Pyridinium Salt of nido-